

Supplementary Material for “Non-Hermitian Photonic Spin-Hall Insulators”

Rodrigo P. Câmara,¹ Tatiana G. Rappoport,^{1,2} and Mário G. Silveirinha¹

¹*Instituto de Telecomunicações, Instituto Superior Técnico,
University of Lisbon, Avenida Rovisco Pais 1, Lisboa, 1049001 Portugal*

²*Instituto de Física, Universidade Federal do Rio de Janeiro,
C.P. 68528, 21941-972 Rio de Janeiro RJ, Brazil*

(Dated: January 5, 2024)

I. PSEUDOSPIN-POLARIZATION IN \mathcal{PD} -SYMMETRIC RECIPROCAL MEDIA

We consider reciprocal electromagnetic systems formed by isotropic materials characterized by the relative permittivity ϵ and permeability μ . For these platforms, the frequency-domain (source-free) Maxwell's equations read

$$\mathbf{M}^{-1} \cdot \begin{pmatrix} \mathbf{0}_{3 \times 3} & ic\nabla \times \mathbf{1}_{3 \times 3} \\ -ic\nabla \times \mathbf{1}_{3 \times 3} & \mathbf{0}_{3 \times 3} \end{pmatrix} \cdot \mathbf{f} = \omega \mathbf{f} \quad \text{with} \quad \mathbf{M}(\mathbf{r}) = \begin{pmatrix} \epsilon(\mathbf{r})\mathbf{1}_{3 \times 3} & \mathbf{0}_{3 \times 3} \\ \mathbf{0}_{3 \times 3} & \mu(\mathbf{r})\mathbf{1}_{3 \times 3} \end{pmatrix}, \quad (\text{S1})$$

where c is the speed of light in vacuum, ω is the oscillation frequency, $\mathbf{r} = (x, y, z)^\top$ is the position vector in a Cartesian reference frame and $\mathbf{f} = (\mathbf{E}, Z_0 \mathbf{H})^\top$ is a 6-vector built from the components of the electromagnetic fields normalized to the same units by means of the vacuum impedance Z_0 . The symbol \cdot denotes the matrix multiplication operation, $^\top$ is the transposition operator and $\mathbf{1}_{3 \times 3}/\mathbf{0}_{3 \times 3}$ are the 3×3 identity/null matrices.

Let us consider that the permittivity and permeability are related as

$$\epsilon(x, y, z) = \mu(x, y, -z). \quad (\text{S2})$$

Then, the eigenvalue problem in Eq.(S1) can be divided into two independent sets of equations [S1]

$$\pm \frac{ic}{\epsilon(z)} \begin{pmatrix} 0 & \partial_z & \partial_y \\ -\partial_z & 0 & -\partial_x \\ \partial_y & -\partial_x & 0 \end{pmatrix} \cdot \Psi^\pm(-z) = \omega \Psi^\pm(z) \quad \text{with} \quad \Psi^\pm(z) = \begin{pmatrix} E_x(z) \mp Z_0 H_x(-z) \\ E_y(z) \mp Z_0 H_y(-z) \\ E_z(z) \pm Z_0 H_z(-z) \end{pmatrix}, \quad (\text{S3})$$

formally equivalent to two decoupled eigenvalue problems $\hat{\mathcal{H}}^\pm \Psi^\pm(z) = \omega \Psi^\pm(z)$. A generic point of space (x, y, z) is denoted as (z) and its mirror-symmetric counterpart $(x, y, -z)$ as $(-z)$ for conciseness. Equation (S3) is nonlocal in space because the left and right hand sides are evaluated at mirror symmetric points. The pseudospinors Ψ^+ and Ψ^- form a basis of solutions of Eq. (S1) which follows from the symmetry of the guide: the electric and parity-transformed magnetic fields are in/out-of phase for the “+”/“−” class. It is important to note that the “pseudospin” degree of freedom is unrelated to the angular momentum (orbital or spin) of the electromagnetic field. It rather refers to the non-local polarization determined by the \mathcal{PD} -symmetry operator. This polarization is the internal degree of freedom that can still convey a topologically nontrivial character to the guide, even though reciprocity renders the global Chern topology trivial. Importantly, the pseudospin decomposition remains valid even when the permittivity and permeability are frequency dependent and complex-valued.

Let $\hat{\mathcal{P}}$ be the parity (mirror) transformation that flips the z -spatial coordinate and $\hat{\mathcal{D}} : (\mathbf{E}, \mathbf{H}) \rightarrow (Z_0 \mathbf{H}, -\mathbf{E}/Z_0)$ be a duality mapping that exchanges the role of the two fields. Both $\hat{\mathcal{P}}$ and $\hat{\mathcal{D}}$ are operators that map the \mathbf{f} -space into itself as $\hat{\mathcal{P}} : \mathbf{f}(z) \rightarrow \mathcal{P} \cdot \mathbf{f}(-z)$ and $\hat{\mathcal{D}} : \mathbf{f}(z) \rightarrow \mathcal{D} \cdot \mathbf{f}(z)$ where [S2]

$$\mathcal{P} = \begin{pmatrix} \mathbf{V} & \mathbf{0}_{3 \times 3} \\ \mathbf{0}_{3 \times 3} & -\mathbf{V} \end{pmatrix} \quad \text{with} \quad \mathbf{V} = \text{diag}(1, 1, -1) \quad \text{and} \quad \mathcal{D} = \begin{pmatrix} \mathbf{0}_{3 \times 3} & \mathbf{1}_{3 \times 3} \\ -\mathbf{1}_{3 \times 3} & \mathbf{0}_{3 \times 3} \end{pmatrix}. \quad (\text{S4})$$

The composition operator

$$\hat{\mathcal{P}} \cdot \hat{\mathcal{D}} : \begin{pmatrix} \mathbf{E}(z) \\ Z_0 \mathbf{H}(z) \end{pmatrix} \rightarrow \begin{pmatrix} Z_0 \mathbf{V} \cdot \mathbf{H}(-z) \\ \mathbf{V} \cdot \mathbf{E}(-z) \end{pmatrix} \quad (\text{S5})$$

maps the Cartesian components of the electric and magnetic fields as $E_z(z) \rightarrow -Z_0 H_z(-z)$, $H_z(z) \rightarrow -E_z(-z)/Z_0$, $E_{x,y}(z) \rightarrow +Z_0 H_{x,y}(-z)$ and $H_{x,y}(z) \rightarrow +E_{x,y}(-z)/Z_0$. It is straightforward to show that for reciprocal isotropic

dielectrics the Maxwell's equations (S1) are $\hat{\mathcal{P}} \cdot \hat{\mathcal{D}}$ symmetric if and only if the permittivity and permeability are linked as in Eq. (S2).

For $\hat{\mathcal{P}} \cdot \hat{\mathcal{D}}$ symmetric reciprocal systems, if \mathbf{f} is a solution of the Maxwell's equations then $\hat{\mathcal{P}} \cdot \hat{\mathcal{D}} \cdot \mathbf{f}$ also is. Because the linear operator $\hat{\mathcal{P}} \cdot \hat{\mathcal{D}}$ satisfies $[\hat{\mathcal{P}} \cdot \hat{\mathcal{D}}]^2 = \mathbf{1}_{6 \times 6}$, the eigenfunctions of the system (S1) can be split into two subsets such that $\hat{\mathcal{P}} \cdot \hat{\mathcal{D}} \cdot \mathbf{f} = \pm \mathbf{f}$. Clearly, Ψ^\pm coincides with the first 3 components of the six-vector $\mathbf{f} \mp \hat{\mathcal{P}} \cdot \hat{\mathcal{D}} \cdot \mathbf{f}$. This property implies that the pseudospinors Ψ^\pm describe the dynamics of the electric field associated with waves with the symmetry $\hat{\mathcal{P}} \cdot \hat{\mathcal{D}} \cdot \mathbf{f} = \mp \mathbf{f}$. Thereby, each pseudospinor symmetry determines itself a solution of the Maxwell's equations with the electric and magnetic fields given by

$$\begin{pmatrix} \mathbf{E}(z) \\ Z_0 \mathbf{H}(z) \end{pmatrix} = \begin{pmatrix} \Psi^\pm(z) \\ \mp \mathbf{V} \cdot \Psi^\pm(-z) \end{pmatrix}. \quad (\text{S6})$$

In the lossless case, when both the permittivity and permeability are real-valued, Eq. (S1) is time-reversal ($\hat{\mathcal{T}}$) invariant. In such a case, the system becomes $\hat{\mathcal{P}} \cdot \hat{\mathcal{T}} \cdot \hat{\mathcal{D}}$ invariant [S2]. The $\hat{\mathcal{P}} \cdot \hat{\mathcal{T}} \cdot \hat{\mathcal{D}}$ operator is anti-linear and satisfies $[\hat{\mathcal{P}} \cdot \hat{\mathcal{T}} \cdot \hat{\mathcal{D}}]^2 = -\mathbf{1}_{6 \times 6}$. Such a formal property allows one to establish a perfect parallelism with the spin-Hall effect and regard the system as a \mathbb{Z}_2 photonic insulator [S2]. The \mathbb{Z}_2 index is written in terms of the topological charge $\mathcal{C}^+ = -\mathcal{C}^-$ of the spin operators $\hat{\mathcal{H}}^\pm$ introduced in the main text. In contrast, in the non-Hermitian case the time-reversal symmetry is broken. Yet, as the system remains reciprocal, it is still possible to guarantee that the two spin operators have opposite topological charge ($\mathcal{C}^+ = -\mathcal{C}^-$), exactly as in the Hermitian case. In this sense, reciprocal $\hat{\mathcal{P}} \cdot \hat{\mathcal{D}}$ systems may be regarded as generalized (non-Hermitian) \mathbb{Z}_2 -photonic insulators.

II. BOUNDARY CONDITIONS FOR THE PPW

The permittivity and permeability of air are related as in Eq. (S2) ($\epsilon(z) = \mu(-z) = 1$). In the parallel-plate waveguide (PPW) schematized in Fig. 1 of the main text, the pseudospin-decomposition can be preserved by choosing plates that are \mathcal{PD} -symmetric. This ensures that the full guide is invariant under a \mathcal{PD} transformation and that the decoupling in Eq. (S3) remains valid [see discussion in Sec. I]. The plates are characterized by a (Leontovich) boundary condition of the form

$$\begin{cases} -Z_+ \hat{\mathbf{z}} \times \mathbf{H}_{\text{tan}}(a/2) = \mathbf{E}_{\text{tan}}(a/2) \\ Z_- \hat{\mathbf{z}} \times \mathbf{H}_{\text{tan}}(-a/2) = \mathbf{E}_{\text{tan}}(-a/2) \end{cases}, \quad (\text{S7})$$

where Z_i is the surface impedance of the $i = +/ -$ (top/bottom, respectively) plate, $\mathbf{E}_{\text{tan}} = \mathbf{E} - \hat{\mathbf{z}}(\hat{\mathbf{z}} \cdot \mathbf{E})$ is the tangential electric field, a is the distance between the plates, \times denotes the cross product between vectors and $\hat{\mathbf{z}}$ is the unitary vector along the positive z -spatial direction. Under a \mathcal{PD} -transformation, the boundary conditions (S7) become

$$\begin{cases} -(Z_0^2/Z_-) \hat{\mathbf{z}} \times \mathbf{H}_{\text{tan}}(a/2) = \mathbf{E}_{\text{tan}}(a/2) \\ (Z_0^2/Z_+) \hat{\mathbf{z}} \times \mathbf{H}_{\text{tan}}(-a/2) = \mathbf{E}_{\text{tan}}(-a/2) \end{cases} \quad (\text{S8})$$

We used the transformation rules for the fields: $(\mathbf{E}_{\text{tan}}(z), \mathbf{H}_{\text{tan}}(z)) \rightarrow (+Z_0 \mathbf{H}_{\text{tan}}(-z), +\mathbf{E}_{\text{tan}}(-z)/Z_0)$, in agreement with Eq. (S5). \mathcal{PD} -invariance requires that (S7) and (S8) must coincide. This is possible when

$$Z_+ Z_- = Z_0^2. \quad (\text{S9})$$

III. BULK MODES

To find the pseudospinor-polarized states Ψ^\pm that propagate in the \mathcal{PD} -symmetric PPW [see Eq. (S3)], we first determine the electromagnetic fields \mathbf{E} and \mathbf{H} that solve Eq. (S1) subject to the boundary conditions in Eq. (S7).

Due to the invariance of the guide under continuous translations in the xy plane, the fields can be factorized as $\mathbf{E}(\mathbf{r}, t) = \mathbf{E}_{\mathbf{k}}(z)e^{-i\omega t}e^{i\mathbf{k}\cdot\mathbf{r}}$ and $\mathbf{H}(\mathbf{r}, t) = \mathbf{H}_{\mathbf{k}}(z)e^{-i\omega t}e^{i\mathbf{k}\cdot\mathbf{r}}$, where \mathbf{k} is the in-plane real-valued wave vector ($\mathbf{k} \cdot \hat{\mathbf{z}} = 0$) with magnitude k . For convenience, first we choose the orientation of the Cartesian reference frame such that $\hat{\mathbf{x}} \cdot \hat{\mathbf{k}} = 1$.

As a starting point, we consider the transverse electric (TE) modes. The *ansatz* $\mathbf{H}_{\mathbf{k}}(z) = h(z)\hat{\mathbf{x}} + \alpha\partial_z h(z)\hat{\mathbf{z}}$ describes a TE field configuration, where α is some coefficient to be determined. The divergence law for magnetism $\nabla \cdot \mathbf{H}(\mathbf{r}, t) = 0$ yields the relation $ikh(z) + \alpha\partial_z^2 h(z) = 0$. On the other hand, it follows from the Helmholtz equation $\nabla^2 H_x + \omega^2 H_x/c^2 = 0$ that $\partial_z^2 h(z) + (\omega^2/c^2 - k^2)h(z) = 0$. Combining both equations one finds that $\alpha \equiv ik/\kappa^2$, where we define the transverse wavenumber $\kappa \equiv \sqrt{\omega^2/c^2 - k^2}$. Using Ampère's law $\nabla \times \mathbf{H} = -i\omega\epsilon_0\mathbf{E}$, one easily finds that the electric field is given by $\mathbf{E}_{\mathbf{k}}(z) = i\frac{\mu_0\omega}{\kappa^2}\partial_z h(z)\hat{\mathbf{y}}$.

The differential equation $\partial_z^2 h(z) + \kappa^2 h(z) = 0$ has the general solution $h(z) = Ae^{i\kappa z} + Be^{-i\kappa z}$, with A and B arbitrary constants. By imposing the boundary conditions (S7), we find that the two coefficients are constrained by:

$$\mathbf{Q} \cdot \begin{pmatrix} A \\ B \end{pmatrix} = 0 \quad \text{with} \quad \mathbf{Q} = \begin{pmatrix} -(\omega/c\kappa - \rho)e^{i\kappa a/2} & (\omega/c\kappa + \rho)e^{-i\kappa a/2} \\ (1 + \rho\omega/c\kappa)e^{-i\kappa a/2} & (1 - \rho\omega/c\kappa)e^{i\kappa a/2} \end{pmatrix}. \quad (\text{S10})$$

We used $Z_{\pm} = \rho^{\pm 1}Z_0$ with ρ real-valued in conformity with Eq. (S9). Non-trivial solutions of the homogeneous linear system must satisfy the modal condition $\det(\mathbf{Q}) = 0$, i.e.,

$$e^{2i\kappa a} = \frac{\omega + c\rho\kappa}{\omega - c\rho\kappa} \frac{\rho\omega + c\kappa}{\rho\omega - c\kappa}, \quad (\text{S11})$$

where $\omega = s \times c\sqrt{k^2 + \kappa^2}$ with the square root branch determined by $s = \pm$. This result shows that the transverse wavenumber is generally a function of k , ρ and a .

In the limit $k \rightarrow 0^+$, Eq. (S11) is analytically solvable and has infinitely many solutions $\kappa_n^{(s=\pm)}$ indexed by $n = 1, 2, \dots$ for both branches $s = \pm$ of the square root [see Sec. VI]. For $0 < k < \infty$, however, Eq. (S11) needs to be numerically solved. To this end, we use the Nelder-Mead minimization scheme [S3]. The Nelder-Mead algorithm is suited to find local minima of a scalar field $f : \mathbb{C} \rightarrow \mathbb{R}$ [S3]. It starts with a set of three points p_0 , q_0 , and s_0 in the complex plane, that form a triangle $\triangle p_0 q_0 s_0$ with centroid c_0 . Then, a composition of N transformations – reflections, expansions, etc. – is applied to the initial triangle, depending on how the values of the function f at the vertices evolve. This produces a series of triangles $\{\triangle p_n q_n s_n\}_n$ with centroids $\{c_n\}_n$ ($n = 0, \dots, N$), such that c_n converges to a local minimum. For this reason, the Nelder-Mead method is also called the downhill simplex method. In our case, we take the function

$$f_k : \mathbb{C} \rightarrow \mathbb{R}_0^+, \quad \kappa \mapsto f_k(\kappa) = \left| e^{2i\kappa a} - \frac{\omega(k, \kappa) + c\rho\kappa}{\omega(k, \kappa) - c\rho\kappa} \frac{\rho\omega(k, \kappa) + c\kappa}{\rho\omega(k, \kappa) - c\kappa} \right|, \quad (\text{S12})$$

with κ the unknown parameter. In the above, $\omega = \omega(k, \kappa)$ represents the function $\omega = s \times c\sqrt{k^2 + \kappa^2}$. We use the Nelder-Mead method recursively, so that κ is calculated for a generic real-valued k , starting from the analytical solution at $k = 0$. In other words, we numerically continue the solution at $k = 0$ to $k > 0$.

From the first identity of the system in Eq. (S10), we find that $B = h_n A$ with $h_n \equiv e^{i\kappa_n a} \frac{\omega_n - c\rho\kappa_n}{\omega_n + c\rho\kappa_n}$. The components of the electromagnetic fields associated with TE modes are thus

$$\begin{cases} H_{\mathbf{k},x}(z) = A(e^{i\kappa_n z} + h_n e^{-i\kappa_n z}) \\ H_{\mathbf{k},z}(z) = -A\frac{k}{\kappa_n}(e^{i\kappa_n z} - h_n e^{-i\kappa_n z}) \\ E_{\mathbf{k},y}(z) = -A\frac{\mu_0\omega_n}{\kappa_n}(e^{i\kappa_n z} - h_n e^{-i\kappa_n z}) \end{cases} \quad (\text{S13})$$

with A being an arbitrary complex number. Using now the projection (S3), one finds that the pseudospinors associated with the TE modes [Eq. (S13)] can be written as $\Psi_n^{\pm}(\mathbf{r}, t) = e^{-i\omega_n t}e^{i\mathbf{k}\cdot\mathbf{r}}\Psi_{\mathbf{k},n}^{\pm}(z)$ with

$$\Psi_{\mathbf{k},n}^{\pm}(z) \propto \begin{pmatrix} \mp(e^{-i\kappa_n z} + h_n e^{i\kappa_n z}) \\ -\frac{\omega_n}{c\kappa_n}(e^{i\kappa_n z} - h_n e^{-i\kappa_n z}) \\ \mp\frac{k}{\kappa_n}(e^{-i\kappa_n z} - h_n e^{i\kappa_n z}) \end{pmatrix}. \quad (\text{S14})$$

Recall that we picked $\hat{\mathbf{x}} \cdot \hat{\mathbf{k}} = 1$. In the general case, the first component of the pseudospinor corresponds to the projection on $\hat{\mathbf{k}}$, the second component corresponds to the projection on $\hat{\mathbf{z}} \times \hat{\mathbf{k}}$, whereas the third component gives the projection on $\hat{\mathbf{z}}$. For completeness, we remark that the transverse magnetic (TM) modes of the PPW lead to the same pseudospinor decomposition.

IV. SPIN CHERN NUMBERS

The electrodynamics in the waveguide is generally not conservative, as there is energy dissipated when $\rho > 0$ and energy pumped into the guide when $\rho < 0$. Non-Hermitian Hamiltonians $\hat{\mathcal{H}} \neq \hat{\mathcal{H}}^\dagger$ describing systems with loss or gain have left ϕ_n^L and right ϕ_n^R eigenstates that, though linked to the same complex eigenenergy E_n , are usually independent [S4]. Here n labels the energy band, $\hat{\mathcal{H}}^\dagger \phi_n^L = E_n^* \phi_n^L$ and $\hat{\mathcal{H}} \phi_n^R = E_n \phi_n^R$. The extension of topological band theory to complex spectra leads to the definition of the Berry potential $\mathcal{A}_{\mathbf{k},n} \equiv i \langle \phi_n^L | \nabla_{\mathbf{k}} \phi_n^R \rangle$ for separable bands, based on the combination of the left and right eigenfunctions [S4]. Here, $\nabla_{\mathbf{k}}$ represents the surface gradient in momentum space and the Dirac notation indicates a suitable inner product. It is supposed that the eigenstates are normalized as $\langle \phi_m^L | \phi_n^R \rangle = \delta_{m,n}$.

In the PPW, switching loss into gain is equivalent to switch the sign of ρ . As a consequence, the operator $\hat{\mathcal{H}}^\dagger$ models a guide with resistivity $-\rho$. This means that $\Psi_n^L(z; \rho) = \Psi_n^R(z; -\rho)$. Thus, the Berry connection can be written as $\mathcal{A}_{\mathbf{k},n}^\pm \equiv i \langle \Psi_{\mathbf{k},n}^\pm(-\rho) | \nabla_{\mathbf{k}} \Psi_{\mathbf{k},n}^\pm(\rho) \rangle$. It is built from properly normalized versions $\Psi_{\mathbf{k},n}^\pm$ of the pseudospinors in Eq. (S14) that satisfy $\langle \Psi_{\mathbf{k},n}^\pm(-\rho) | \Psi_{\mathbf{k},n}^\pm(\rho) \rangle = 1$. We choose $\langle \mathbf{F} | \mathbf{Q} \rangle = \int_{-a/2}^{a/2} dz \mathbf{F}^\dagger(z) \cdot \mathbf{Q}(z)$ as the inner product of any two vectors \mathbf{F} and \mathbf{Q} . Note that the Berry potential is independent of the z -spatial coordinate.

The Chern number \mathcal{C}_n^\pm is the topological invariant determined by the integral of the Berry curvature $\nabla_{\mathbf{k}} \times \mathcal{A}_{\mathbf{k},n}^\pm$ over the momentum space, i.e., the Euclidean plane (\mathbf{k} is a generic vector in the xy plane). Stokes theorem tells us that [S5]

$$\mathcal{C}_n^\pm = (2\pi)^{-1} \left[\lim_{k \rightarrow \infty} - \lim_{k \rightarrow 0^+} \right] k \int_0^{2\pi} d\phi \mathcal{A}_{\phi,n}^\pm \quad \text{with} \quad \mathcal{A}_{\phi,n}^\pm = \mathcal{A}_{\mathbf{k},n}^\pm \cdot \hat{\phi}, \quad (\text{S15})$$

provided that the Berry potential is smooth for $k \in]0, \infty[$. Here, $\mathbf{k} = (k, \phi) \in [0, \infty[\times [0, 2\pi[$ is associated with a system of polar coordinates of the momentum space so that $\nabla_{\mathbf{k}} = \hat{\mathbf{k}} \partial_k + \hat{\phi} k^{-1} \partial_\phi$. It is implicit that we adopt a gauge such that the eigenfunctions $\Psi_{\mathbf{k},n}^\pm$ are invariant under arbitrary rotations around the z -axis, consistent with the continuous rotation symmetry of the PPW. Thus, the components of the states $\Psi_{\mathbf{k},n}^\pm$ in Eq.(S14) are independent of the ϕ coordinate. As a result, $\mathcal{A}_{\phi,n}^\pm$ in Eq. (S15) is also independent of ϕ , and the Chern number becomes $\mathcal{C}_n^\pm = [\lim_{k \rightarrow \infty} - \lim_{k \rightarrow 0^+}] k \mathcal{A}_{\phi,n}^\pm$. Taking into account the normalization of the eigenfunctions, the azimuthal component of the Berry potential $\mathcal{A}_{\phi,n}^\pm$ can be written as

$$\mathcal{A}_{\phi,n}^\pm = ik^{-1} \frac{\langle \Psi_{\mathbf{k},n}^\pm(-\rho) | \partial_\phi \Psi_{\mathbf{k},n}^\pm(\rho) \rangle}{\langle \Psi_{\mathbf{k},n}^\pm(-\rho) | \Psi_{\mathbf{k},n}^\pm(\rho) \rangle}. \quad (\text{S16})$$

Making use of the symmetries $\kappa_n(k; -\rho) = \kappa_n^*(k; \rho)$, $\omega_n(k; -\rho) = \omega_n^*(k; \rho)$ of the modal Eq.(S11), the denominator can be determined from Eq. (S14) as

$$\begin{aligned} \langle \Psi_{\mathbf{k},n}^\pm(-\rho) | \Psi_{\mathbf{k},n}^\pm(\rho) \rangle A^{-2} Z_0^{-2} &= \int_{-a/2}^{a/2} dz \begin{pmatrix} \mp (e^{-i\kappa_n^* z} + h_n^* e^{i\kappa_n^* z}) \\ -\frac{\omega_n^*}{c\kappa_n^*} (e^{i\kappa_n^* z} - h_n^* e^{-i\kappa_n^* z}) \\ \mp \frac{k}{\kappa_n^*} (e^{-i\kappa_n^* z} - h_n^* e^{i\kappa_n^* z}) \end{pmatrix}^\dagger \cdot \begin{pmatrix} \mp (e^{-i\kappa_n z} + h_n e^{i\kappa_n z}) \\ -\frac{\omega_n}{c\kappa_n} (e^{i\kappa_n z} - h_n e^{-i\kappa_n z}) \\ \mp \frac{k}{\kappa_n} (e^{-i\kappa_n z} - h_n e^{i\kappa_n z}) \end{pmatrix} \\ &= \frac{4a\omega_n^2}{c^2\kappa_n^2} + \frac{ik^2}{\kappa_n^3} (e^{i\kappa_n a} - e^{-i\kappa_n a}) (h_n + h_n^{-1}). \end{aligned} \quad (\text{S17})$$

Next, we turn our attention to the numerator of Eq.(S16). We note that ∂_ϕ can only act on the vector basis $(\hat{\mathbf{k}}, \hat{\phi}, \hat{\mathbf{z}})$. Using $\partial_\phi \hat{\mathbf{k}} = \hat{\phi}$, $\partial_\phi \hat{\phi} = -\hat{\mathbf{k}}$ and $\partial_\phi \hat{\mathbf{z}} = 0$, it is found that:

$$\begin{aligned} \langle \Psi_{\mathbf{k},n}^\pm(-\rho) | \partial_\phi \Psi_{\mathbf{k},n}^\pm(\rho) \rangle A^{-2} Z_0^{-2} &= \int_{-a/2}^{a/2} dz \begin{pmatrix} \mp (e^{-i\kappa_n^* z} + h_n^* e^{i\kappa_n^* z}) \\ -\frac{\omega_n^*}{c\kappa_n^*} (e^{i\kappa_n^* z} - h_n^* e^{-i\kappa_n^* z}) \\ \mp \frac{k}{\kappa_n^*} (e^{-i\kappa_n^* z} - h_n^* e^{i\kappa_n^* z}) \end{pmatrix}^\dagger \begin{pmatrix} \frac{\omega_n}{c\kappa_n} (e^{i\kappa_n z} - h_n e^{-i\kappa_n z}) \\ \mp (e^{-i\kappa_n z} + h_n e^{i\kappa_n z}) \\ 0 \end{pmatrix} \\ &= \pm \frac{2a\omega_n}{c\kappa_n} (h_n - h_n^{-1}). \end{aligned} \quad (\text{S18})$$

Hence, the Berry potential can be explicitly written as:

$$k\mathcal{A}_{\phi,n}^{\pm} = \pm i \frac{2a\omega_n}{c\kappa_n} (h_n - h_n^{-1}) \left[\frac{4a\omega_n^2}{c^2\kappa_n^2} + \frac{ik^2}{\kappa_n^3} (e^{i\kappa_n a} - e^{-i\kappa_n a}) (h_n + h_n^{-1}) \right]^{-1}. \quad (\text{S19})$$

In order to obtain the Chern numbers from Eqs. (S15) and (S19), it is necessary to evaluate $e^{i\kappa_n a}$ and h_n in the limits $k \rightarrow 0^+$ and $k \rightarrow \infty$. Such analysis is reported in Sec. VI. Using Eqs. (S29) and (S30) we find that:

$$\lim_{k \rightarrow \infty} k\mathcal{A}_{\phi,n}^{\pm} = 0 \quad \text{and} \quad \lim_{k \rightarrow 0^+} k\mathcal{A}_{\phi,n}^{\pm} = \mp s \times (-1)^{n+1} \text{sgn}(1 - |\rho|) \quad (\text{S20})$$

for all resistivity values $\rho \in \mathbb{R} \setminus \{-1, 1\}$ for which the n -th band is separable from the rest of the spectrum and the Berry potential is smooth in $k \in]0, \infty[$. The sign \pm specifies the up/down polarization of the pseudospinors and $s = \pm$ the square root branch. As a result,

$$\mathcal{C}_n^{\pm} = \pm s \times (-1)^{n+1} \text{sgn}(1 - |\rho|). \quad (\text{S21})$$

Despite the focus on non-conservative PPWs, the $\rho = 0$ case is also accounted for in the previous calculations. In fact, the biorthogonal system of left and right eigenstates can still be found for conservative models with $\hat{\mathcal{H}} = \hat{\mathcal{H}}^\dagger$. Evidently, for a conservative system, $\phi_n^L = \phi_n^R$, and in such a case we recover the Hermitian formulation of topological band theory.

When the plates are interchanged in the guide ($\rho \rightarrow \rho^{-1}$), Eq. (S11) is left invariant. Thus, it still determines the transverse wavenumbers κ_n and natural frequencies ω_n in the transformed system. However, the weight h_n relating the coefficients of the scalar function $h(z) = Ae^{i\kappa_n z} + Be^{-i\kappa_n z}$ as $B = h_n A$ transforms as $h_n \rightarrow h_n^{-1}$. According to Eqs. (S17) and (S18), the azimuthal component of the Berry potential $\mathcal{A}_{\phi,n}^{\pm}$ must then invert its sign in the new guide, $\mathcal{A}_{\phi,n}^{\pm} \rightarrow -\mathcal{A}_{\phi,n}^{\pm}$. This means that the spin Chern numbers (for the same frequency band) in two waveguides related by parity-symmetry have opposite signs.

It is useful to analyze the asymptotic properties of the pseudospinors $\Psi_{\mathbf{k},n}^{\pm}$ given by Eq. (S14). In the limit $k \rightarrow \infty$, κ_n and h_n are finite, but the frequency ω_n diverges [see Sec. VI]. Therefore, the projection of the pseudospinor along $\hat{\mathbf{k}}$ is negligible when compared to the other components:

$$\Psi_{\mathbf{k},n}^{\pm}(z) = 2iAZ_0 e^{i\kappa_n a/2} \begin{pmatrix} 0 \\ -\frac{\omega_n}{c\kappa_n} \sin[\kappa_n(z - a/2)] \\ \pm \frac{k}{\kappa_n} \sin[\kappa_n(z + a/2)] \end{pmatrix}. \quad (\text{S22})$$

Apart from a global phase, the Ψ^{\pm} spinor components are all real-valued resulting in $\lim_{k \rightarrow \infty} k\mathcal{A}_{\phi,n}^{\pm} = 0$, in agreement with Eq. (S20).

V. PARTICLE-HOLE SYMMETRY IN PHOTONICS

Because the electromagnetic field is real-valued, the positive and negative frequency spectra must be balanced in photonic platforms. Specifically, if there is a mode with a time variation of the type $e^{-i\omega t}$, then it has a partner with time variation $e^{+i\omega^* t}$. Thereby, the spectrum of photonic systems is constrained by the particle-hole symmetry $\omega(\mathbf{k}) = -\omega^*(\mathbf{k})$, following the terminology commonly adopted in topological photonics.

In our parallel-plate waveguide, the boundary conditions determine an infinite number of modes with positive frequencies ($\omega' > 0$) for any fixed \mathbf{k} . The particle-hole symmetry then requires the existence of an infinite number of modes with negative frequencies ($\omega' < 0$) and wave vector $-\mathbf{k}$. The result is that our gapped systems are characterized by an infinite number of bands below the zero-frequency band gap. Thus, unlike electronic platforms, our guide has no ground state [see Fig. S1]. In this situation, the standard methods of topology may breakdown [S6]. In Sec. VIII, we shall show that even though our system has no "ground" it is still possible to use the Chern numbers of the individual bands to predict the emergence of protected edge states.

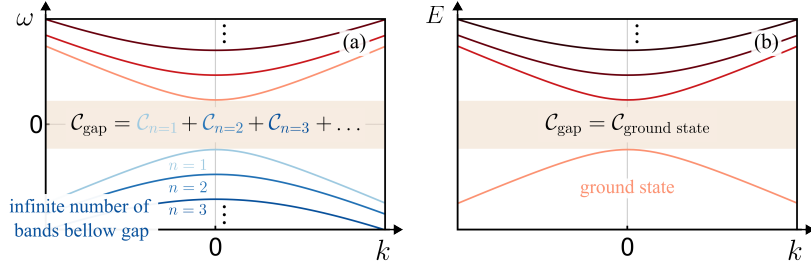


FIG. S1. Schematic band structures of conservative (a) photonic and (b) electronic systems. Different from the electronic case, typically the photonic spectrum has an infinite number of bands below the gap due to the particle-hole symmetry. Hence, there is no ground state. The gap Chern number is determined by the sum of all the Chern numbers of all bands below the gap. For the photonic case, \mathcal{C}_{gap} is given by an infinite sum of integers, and thus it may be ill-defined [S6].

VI. USEFUL LIMITS

For convenience we decompose the transverse wavenumber and frequency into real and imaginary components: $\kappa_n = \kappa'_n + i\kappa''_n$ and $\omega_n = \omega'_n + i\omega''_n$. When $k = 0$, the modal equation (S11) takes the form

$$\begin{aligned} \lim_{k \rightarrow 0^+} e^{2i\kappa_n a} &= \lim_{k \rightarrow 0^+} \frac{s \times \sqrt{k^2 + \kappa_n^2} + \rho \kappa_n}{s \times \sqrt{k^2 + \kappa_n^2} - \rho \kappa_n} \frac{s \times \sqrt{k^2 + \kappa_n^2} \rho + \kappa_n}{s \times \sqrt{k^2 + \kappa_n^2} \rho - \kappa_n} = - \left| \frac{s \times \rho + 1}{s \times \rho - 1} \right|^2 \\ &= \exp \left(2i \left[\frac{\pi}{2a} (2n - 1) - s \times i \frac{\mathcal{F}(\rho)}{a} \right] a \right) \quad \text{with} \quad \mathcal{F}(\rho) \equiv \text{sgn}(\rho) \ln \left| \frac{|\rho| + 1}{|\rho| - 1} \right| \end{aligned} \quad (\text{S23})$$

and $n \in \mathbb{N}$. The sign $s = \pm$ selects the square root branch and is omitted for clarity ($\kappa_n^{(s=\pm)} \rightarrow \kappa_n$). Without loss of generality, we take $\kappa'_n > 0$. Evidently,

$$\kappa_n^{(s=\pm)}(k=0) = \frac{\pi}{2a} (2n - 1) - s \times i \frac{\mathcal{F}(\rho)}{a}. \quad (\text{S24})$$

On the other hand, in the $k \rightarrow \infty$ limit with $\rho \neq 0$, the modal equation (S11) becomes

$$e^{2i\kappa_m a} = 1 \quad (k \rightarrow \infty \quad \text{with} \quad \rho \neq 0). \quad (\text{S25})$$

As a result, it follows that

$$\kappa_m^{(s=\pm)}(k \rightarrow \infty; \rho \neq 0) \rightarrow \frac{\pi}{2a} 2m \quad \text{with} \quad m \in \mathbb{N}. \quad (\text{S26})$$

Numerical calculations show that the solutions labeled by index n in Eq.(S24) are analytically continued to the solutions of (S26) with $m = n$. Thus, we can write

$$\kappa_n^{(s=\pm)}(k \rightarrow \infty; \rho \neq 0) \rightarrow \frac{\pi}{2a} 2n. \quad (\text{S27})$$

Here, $\kappa_n(k)$ ($0 \leq k < \infty$) represents the n -th transverse wavenumber band of the waveguide.

For completeness, we note that when $\rho = 0$, the modal equation (S11) becomes independent of k , and reduces to $e^{2i\kappa_n a} = -1$. The corresponding transverse wavenumbers are $\kappa_n^{(s=\pm)}(k; \rho = 0) = \frac{\pi}{2a} (2n - 1)$ with $n \in \mathbb{N}$, and match the $k = 0$ solutions in Eq.(S24) with $\mathcal{F}(\rho = 0)$.

From Eq. (S27), it is evident that the asymptotic form of the eigenfrequencies is ruled by

$$\lim_{k \rightarrow \infty} \omega_n^{(s=\pm)}(k) = \lim_{k \rightarrow \infty} s \times ck. \quad (\text{S28})$$

The preceding results can be used to determine $e^{i\kappa_n a}$ and $h_n = e^{i\kappa_n a} \frac{\omega_n - c\rho\kappa_n}{\omega_n + c\rho\kappa_n}$ in the limits $k \rightarrow 0^+$ and $k \rightarrow \infty$. These limits are useful to evaluate Chern numbers in Eq. (S21). Straightforward calculations show that

$$\lim_{k \rightarrow \infty, \rho \neq 0} e^{i\kappa_n a} = \lim_{k \rightarrow \infty, \rho \neq 0} h_n = (-1)^n \quad \text{and} \quad \lim_{k \rightarrow \infty, \rho = 0} e^{i\kappa_n a} = \lim_{k \rightarrow \infty, \rho = 0} h_n = i(-1)^{n+1} \quad (\text{S29})$$

and

$$\lim_{k \rightarrow 0^+} e^{i\kappa_n^{(s=\pm)} a} = i(-1)^{n+1} \left| \frac{|\rho| + 1}{|\rho| - 1} \right|^{s \times \text{sgn}(\rho)} \quad \text{and} \quad \lim_{k \rightarrow 0^+} h_n = i(-1)^{n+1} \text{sgn}(1 - |\rho|). \quad (\text{S30})$$

VII. BAND STRUCTURE NEAR THE PHASE TRANSITION

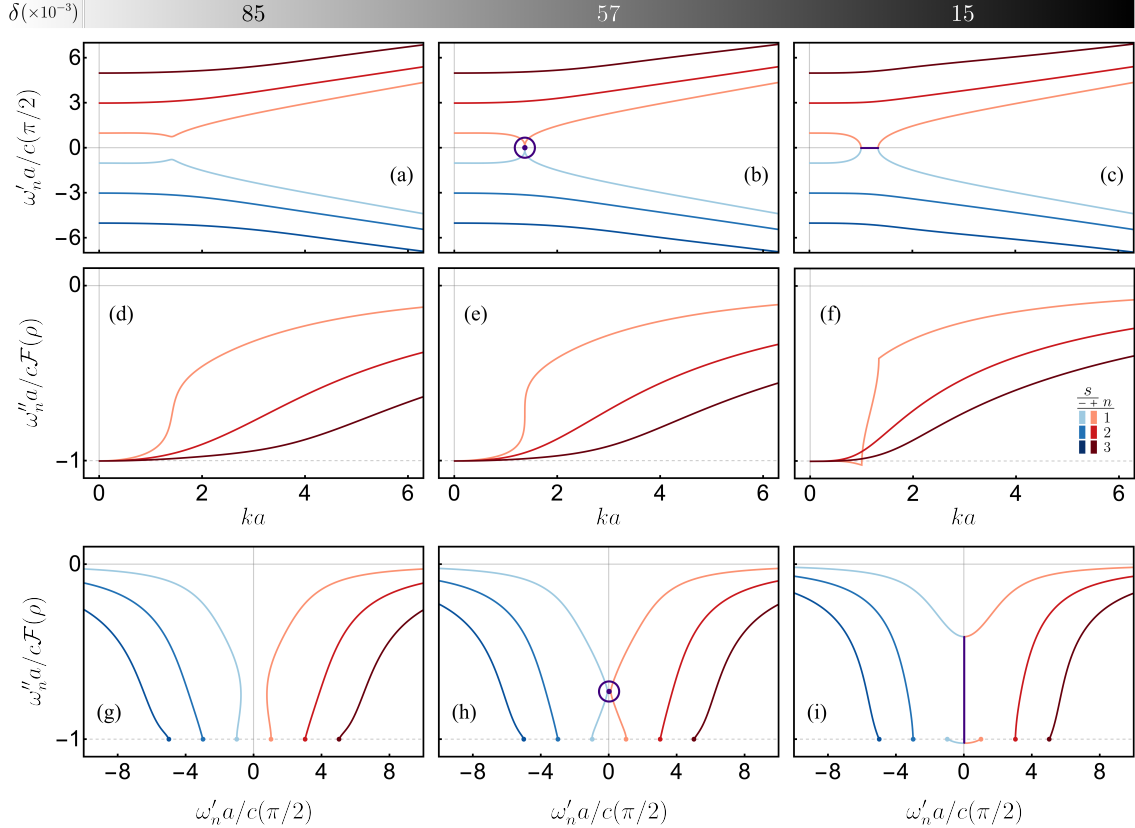


FIG. S2. (a, b, c) Real ω'_n and (d, e, f) imaginary ω''_n components of the frequency bands as functions of the in-plane momentum magnitude k , for $n \in \{1, 2, 3\}$ and both signs of the square root $s = \pm$. The branches $\omega_n^{(s=+)''}$ and $\omega_n^{(s=-)''}$ coincide in (d, e, f). (g, h, i) Locus of the band structure in the complex plane. The resistivity ρ is determined by (g) $\delta = 85 \times 10^{-3}$, (h) $\delta = 57 \times 10^{-3}$ and (i) $\delta = 15 \times 10^{-3}$ with $\rho = 1 - \delta$. The degeneracies between square root branches are indicated in purple.

In Figs. 2(c), 2(d) and 2(e) of the main text, the lowest-order frequency bands of propagating modes inside the PPW are projected onto the complex plane for three values of $\delta = 1 - |\rho|$ near the critical resistivity $\rho = 1$. Each curve represents the locus in the complex-plane of $\omega_{n=1}^{(s=\pm)}(k)$ for all k real-valued and a fixed square root sign $s = \pm$. For a better understanding of how the frequency solutions evolve with the in-plane momentum magnitude, the real and imaginary components ω'_n and ω''_n are shown separately as functions of k in Fig. S2, not only for the $n = 1$ bands, but also for the bands $n = 2$ and $n = 3$.

In Supplementary Movie 1, we present the evolution of the band structure in the complex plane as the resistivity varies continuously from $\rho = 0.762$ to $\rho = 0.987$. The positive ($s = +$) and negative ($s = -$) bands are displayed for $n = 1, 2, 3$. The coalescence of the $n = 1$ bands is highlighted in purple after the resistivity crosses the critical value $\rho = 0.9434$. For a better understanding of the dependence on ρ , the imaginary parts $\omega_n^{(s=\pm)''}$ are not normalized to $\mathcal{F}(\rho)$ in the supplementary movie. The frequency loci at $k = 0$ are represented by solid dots.

VIII. EDGE STATES OF THE PEC-PMC GUIDE TERMINATED BY AN OPAQUE WALL

Suppose that the PPW with a PEC plate on the top and a PMC plate on the bottom is terminated by an arbitrarily shaped curved vertical wall [see Fig. S3(a)]. The unit vector $\hat{\mathbf{n}}$ normal to the wall lies on the xoy -plane ($\hat{\mathbf{n}} \cdot \hat{\mathbf{z}} = 0$) and is a function of the position on the wall. $\hat{\mathbf{n}}$ points to the interior of the guide.

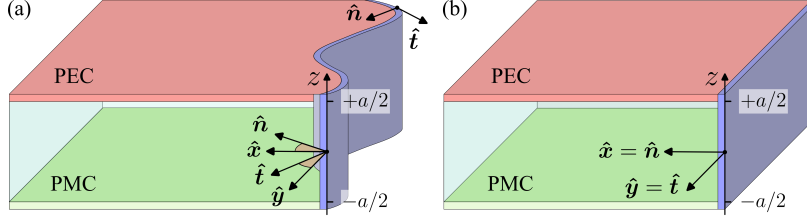


FIG. S3. Sketch of the PEC-PMC waveguide terminated with an opaque lateral wall (purple). (a) Arbitrarily shaped-vertical wall. The normal and tangent unit vectors to the wall, $\hat{\mathbf{n}}$ and $\hat{\mathbf{t}}$, are functions of the position on the wall, but everywhere perpendicular to the z -axis. (b) Straight edge. In this case, $\hat{\mathbf{n}}$ and $\hat{\mathbf{t}}$ are constant and coincide with the unit vectors of the basis of the xoy -plane.

A. Anisotropic and \mathcal{PTD} -Symmetric Curved Lateral Wall

We consider that the wall is characterized by an anisotropic surface impedance, so that the electric and magnetic fields satisfy the Leontovich boundary condition

$$\mathbf{Z} \cdot (\hat{\mathbf{n}} \times \mathbf{H}_{\text{tan}}) = \mathbf{E}_{\text{tan}}, \quad (\text{S31})$$

where $\mathbf{F}_{\text{tan}} = \mathbf{F} - (\mathbf{F} \cdot \hat{\mathbf{n}}) \hat{\mathbf{n}}$ is the tangential field ($\mathbf{F} \in \{\mathbf{E}, \mathbf{H}\}$) and $\mathbf{Z} = Z_{\parallel} \hat{\mathbf{t}} \otimes \hat{\mathbf{t}} + Z_z \hat{\mathbf{z}} \otimes \hat{\mathbf{z}}$ is the surface impedance. Here, \otimes denotes the tensor product of two vectors. Anisotropic surface impedances can be implemented using corrugated conducting plates [S7, S8]. In particular, surfaces such that one of the components Z_{\parallel} or Z_z vanishes and the other diverges to infinity mimic soft or hard acoustic scatterers in electromagnetics [S7, S8]. Here, we consider the general case where the impedances are finite and dispersive.

The components Z_{\parallel} or Z_z are constrained by \mathcal{PD} -symmetry. As the surface impedance of the lateral wall is independent of z , one sees from Eq. (S5) that the Leontovich boundary condition is compatible with the \mathcal{PD} -symmetry of the guide only if $\mathbf{Z} \cdot (\hat{\mathbf{n}} \times [Z_0^{-1} \mathbf{V} \cdot \mathbf{E}]_{\text{tan}}) = [Z_0 \mathbf{V} \cdot \mathbf{H}]_{\text{tan}}$. It is straightforward to check that this condition is consistent with (S31) if and only if

$$Z_{\parallel} Z_z = Z_0^2. \quad (\text{S32})$$

Thus, the \mathcal{PD} -invariance of the lateral wall requires that the surface impedance components satisfy the above constraint. In the Hermitian case, the impedances Z_{\parallel} or Z_z are pure imaginary numbers, so that both the wall and bulk region are \mathcal{PTD} -symmetric.

Using Eq. (S6), we may write the boundary condition (S31) in terms of the pseudospinors. Interestingly, under the constraint (S32), the pseudospinors satisfy a single scalar constraint on the lateral wall:

$$\Psi_z^{\pm}(z) = \mp (Z_z/Z_0) \Psi_t^{\pm}(-z). \quad (\text{S33})$$

The subscripts z and t refer to the pseudospinor components in the right-handed orthogonal basis $(\hat{\mathbf{n}}, \hat{\mathbf{t}}, \hat{\mathbf{z}})$.

B. Hamiltonian Decomposition

Next, we show that the bulk label n remains a good “quantum number” for the modes of the electromagnetic field, even in the presence of the boundary wall. In other words, the curved wall does not mix bulk modes with different n in our problem.

To demonstrate this, we look for excitations of the electromagnetic field such that the dependence on z is separable from the dependence on x and y , for all the field components. This is possible because the wall is vertical ($\hat{\mathbf{n}} \cdot \hat{\mathbf{z}} = 0$) and the surface impedance is independent of the z -spatial coordinate. Specifically, inspired by the structure of bulk modes with index n in a PEC-PMC guide, we pick the following field *ansatz*

$$\Psi_n^\pm(\mathbf{r}, t) := \begin{pmatrix} \sin[\kappa_n(z - a/2)] \psi_x(x, y) \\ \sin[\kappa_n(z - a/2)] \psi_y(x, y) \\ \cos[\kappa_n(z - a/2)] \psi_z(x, y) \end{pmatrix} e^{-i\omega t} \quad \text{with} \quad \kappa_n = (2n - 1) \frac{\pi}{2a} \quad n \in \mathbb{N}, \quad (\text{S34})$$

Note that we use the values of the transverse wavenumber κ_n found in Sec. VI for a conservative ($\rho = 0$) guide. The *ansatz* automatically guarantees that the boundary conditions on the top/bottom walls of the waveguide are satisfied. Indeed, as the electric/magnetic fields tangential to the PEC/PMC plate must vanish we need that: $E_x(a/2) = E_y(a/2) = 0$ and $H_x(-a/2) = H_y(-a/2) = 0$. We use the shorthand notation $F(\pm a/2) \equiv F(z = \pm a/2)$. From Eq. (S6) it follows that these boundary constraints may be written in terms of the pseudospinors simply as $\Psi_x(a/2) = \Psi_y(a/2) = 0$, which is trivially satisfied by our *ansatz* because $\sin 0 = 0$.

Feeding the pseudospinors in Eq. (S34) into the Maxwell's equations (S3) leads to

$$\pm i \begin{pmatrix} \cos[\kappa_n(z + a/2)] (-\kappa_n \psi_y + \partial_y \psi_z) \\ \cos[\kappa_n(z + a/2)] (\kappa_n \psi_x - \partial_x \psi_z) \\ \sin[\kappa_n(z + a/2)] (-\partial_y \psi_x + \partial_x \psi_y) \end{pmatrix} = \frac{\omega}{c} \begin{pmatrix} \sin[\kappa_n(z - a/2)] \psi_x \\ \sin[\kappa_n(z - a/2)] \psi_y \\ \cos[\kappa_n(z - a/2)] \psi_z \end{pmatrix}. \quad (\text{S35})$$

Since

$$\cos[\kappa_n(z + a/2)] = (-1)^n \sin[\kappa_n(z - a/2)] \quad \text{and} \quad \sin[\kappa_n(z + a/2)] = (-1)^{n+1} \cos[\kappa_n(z - a/2)], \quad (\text{S36})$$

the functions of z on each side of Eq. (S35) can be matched componentwise. Hence, we find

$$\underbrace{\pm i (-1)^n \begin{pmatrix} 0 & -\kappa_n & \partial_y \\ \kappa_n & 0 & -\partial_x \\ \partial_y & -\partial_x & 0 \end{pmatrix}}_{\equiv \hat{\mathcal{H}}_n^\pm} \psi(x, y) = \frac{\omega}{c} \psi(x, y) \quad \text{with} \quad \psi(x, y) = \begin{pmatrix} \psi_x(x, y) \\ \psi_y(x, y) \\ \psi_z(x, y) \end{pmatrix}, \quad (\text{S37})$$

i.e., an equation for the vector ψ alone.

The last step to demonstrate that n remains a good quantum number is to show that the *ansatz* is compatible with the boundary condition on the lateral wall (S33). Feeding Eq. (S34) into Eq. (S33) leads to

$$\cos[\kappa_n(z - a/2)] \hat{\mathbf{z}} \cdot \psi = \pm \frac{Z_z}{Z_0} \sin[\kappa_n(z + a/2)] \hat{\mathbf{t}} \cdot \psi. \quad (\text{S38})$$

The z dependence on both sides of the above equation is compatible due to Eq. (S36). Therefore, the boundary constraint on the anisotropic and \mathcal{PTD} -symmetric lateral wall reduces to

$$\hat{\mathbf{z}} \cdot \psi = \pm i \chi_z (-1)^n \hat{\mathbf{t}} \cdot \psi, \quad (\text{S39})$$

with $\chi_z = iZ_z/Z_0$ the real-valued normalized reactance along the z -direction. This last result confirms that the lateral wall does not couple bulk modes associated with different quantum numbers n .

The previous analysis shows that the global Hamiltonian can be written as the direct sum of the Hamiltonians of the waves with quantum number n . This property is illustrated pictorially in Fig. S4. The figure represents the band structure of each Hamiltonian-component in the bulk-region. However, it is crucial to note that the decomposition is not restricted to bulk modes, but it still holds true when the waveguide is terminated by the anisotropic and \mathcal{PTD} -symmetric wall. Indeed, as previously noted, the wall does not couple pseudospinors labelled by different integers. Thereby, the eigenspaces generated by the waves with quantum number n do not mix. Our system is effectively equivalent to an infinite set of totally decoupled waveguides, each described by an operator $\hat{\mathcal{H}}_n^\pm$. In particular, our analysis demonstrates that the edge states with quantum number n that propagate confined to the lateral wall do not scatter into other modes (labelled by $m \neq n$), regardless of the shape of the interface.

Let us now focus on the Hamiltonian of the pseudospin class “+”. From the previous discussion, it may be decomposed as follows:

$$\hat{\mathcal{H}}^+ = \hat{\mathcal{H}}_1^+ \oplus \hat{\mathcal{H}}_2^+ \oplus \cdots = \bigoplus_{n \in \mathbb{N}} \hat{\mathcal{H}}_n^+, \quad (\text{S40})$$

where $\hat{\mathcal{H}}_n^+$ is the operator defined in Eq. (S37), which rules the waves with quantum number n with the field structure shown in Eq. (S34). As illustrated in Fig. S4, $\hat{\mathcal{H}}_n^+$ describes a two-band system. Hence, it has a single band below the gap, and its topology is well-defined. In particular, the number of edge states associated with the quantum number n can be predicted using the bulk-edge correspondence. The implications of this property will be further discussed in the next subsection.

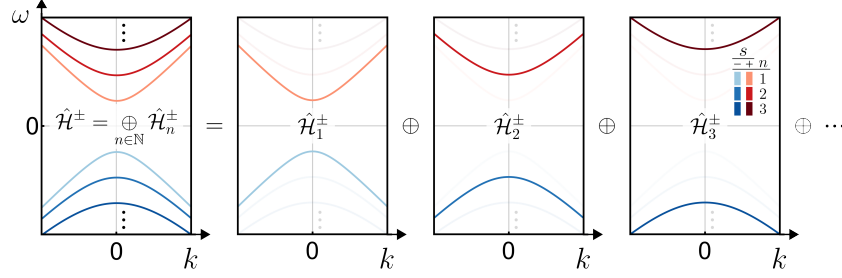


FIG. S4. Illustration of the Hamiltonian decomposition in Eq. (S40). The Hamiltonian of the edge waveguide $\hat{\mathcal{H}}^\pm$ is the direct sum of two-band Hamiltonians $\hat{\mathcal{H}}_n^\pm$ that act each only on the pseudospinors with quantum number n .

For completeness, it is interesting to note that the system of differential equations (S37) is equivalent to solving the Helmholtz equation

$$-(\partial_x^2 + \partial_y^2) \psi_z = \left(\frac{\omega^2}{c^2} - \kappa_n^2 \right) \psi_z \quad (\text{S41})$$

for the z -component of ψ , with the remaining ones given by

$$\begin{cases} \psi_x = \left(\frac{\omega}{c} - \frac{\kappa_n c}{\omega} \right)^{-1} \left(-\frac{\kappa_n c}{\omega} \partial_x \pm i(-1)^n \partial_y \right) \psi_z \\ \psi_y = \left(\frac{\omega}{c} - \frac{\kappa_n c}{\omega} \right)^{-1} \left(-\frac{\kappa_n c}{\omega} \partial_y \mp i(-1)^n \partial_x \right) \psi_z \end{cases} \quad (\text{S42})$$

Thus, we have reduced the task of solving Maxwell's equations inside the PPW to a 2-dimensional problem.

C. Edge States for a Straight Lateral Wall

For the case of a straight edge, we can deduce the dispersion relation of edge states analytically. We suppose that the lateral wall is defined by $x = 0$, so that the edge mode propagates along the y -axis as illustrated in Fig. S3(b). For this setup, the tangential unit vector is constant along the wall, $\hat{\mathbf{t}} = \hat{\mathbf{y}}$. We take

$$\psi_z = e^{i\mathbf{k} \cdot \mathbf{r}}, \quad (\text{S43})$$

with $\mathbf{k} = k_x \hat{\mathbf{x}} + k_y \hat{\mathbf{y}}$ the in-plane wave vector. The pseudospinor component ψ_z is a solution of the Helmholtz equation (S41) with $\omega_n^2/c^2 = \kappa_n^2 + k^2$ ($k^2 \equiv k_x^2 + k_y^2$). The x and y components of the vector ψ follow from Eq. (S42) and read

$$\begin{cases} \psi_x = \left(-i \frac{\kappa_n}{k^2} k_x \mp (-1)^n \frac{\omega_n}{ck^2} k_y \right) e^{i\mathbf{k} \cdot \mathbf{r}} \\ \psi_y = \left(-i \frac{\kappa_n}{k^2} k_y \pm (-1)^n \frac{\omega_n}{ck^2} k_x \right) e^{i\mathbf{k} \cdot \mathbf{r}} \end{cases} \quad (\text{S44})$$

Note that $\psi_{x,y,z} \propto e^{i\mathbf{k}\cdot\mathbf{r}}$, so that the pseudospinors in Eq. (S34) are ruled by the propagation factor $\Psi_n^\pm \propto e^{i\mathbf{k}\cdot\mathbf{r}}$, similar to the bulk modes of the main text. We feed the components ψ_z and ψ_y in Eqs. (S43) and (S44) to the boundary constraint in Eq. (S39) with $\hat{\mathbf{t}} = \hat{\mathbf{y}}$ to find that

$$\frac{k^2}{\kappa_n} = \chi_z \left(\pm(-1)^n k_y + i \frac{\omega_n}{c\kappa_n} k_x \right). \quad (\text{S45})$$

We are interested in edge waves that propagate attached to the lateral wall. Therefore, it is assumed that k_y and $\alpha_x \equiv -ik_x = \sqrt{k_y^2 + \kappa_n^2 - \omega_n^2/c^2}$ are real-valued propagation and attenuation constants, so that the pseudospinors vary on the xoy -plane as $\Psi_n^\pm \sim e^{ik_y y} e^{-\alpha_x x}$. In these conditions, the dispersion of the edge modes with quantum number n [Eq. (S45)] reduces to:

$$\frac{\omega_n^2/c^2 - \kappa_n^2}{\kappa_n} = \chi_z \left(\pm(-1)^n k_y - \frac{\omega_n}{c\kappa_n} \sqrt{k_y^2 + \kappa_n^2 - \omega_n^2/c^2} \right). \quad (\text{S46})$$

To illustrate the discussion, we show in Fig. S5 the frequency bands ω_n of the edge waves as a function of the propagation constant k_y , for $n < 5$. We take $\chi_z = 0.12\omega a/c$, which corresponds to an inductive Z_z and a capacitive Z_\parallel . It is clear that the edged waveguide supports an *infinite* number of edge waves that propagate alternately to the $+y$ and $-y$ directions, depending on the quantum number n . Besides, the edge waves associated with the Hamiltonians $\hat{\mathcal{H}}_n^+$ and $\hat{\mathcal{H}}_n^-$ propagate in opposite directions. A final key observation is that the edge modes are gapless: $\lim_{k_y \rightarrow \pm\infty} \omega_n = 0$.

The properties of the edge transport discussed above and illustrated by Fig. S5 are in precise agreement with the topological character of the waveguide. As already discussed in Sec. VIII B, the Hamiltonian $\hat{\mathcal{H}}^+$ is a direct sum of partial two-band Hamiltonians $\hat{\mathcal{H}}_n^+$ that act on the pseudospinors with quantum number n [see Eq. (S40)]. Each Hamiltonian $\hat{\mathcal{H}}_n^+$ has a single (negative) frequency band below the gap [see Fig. S4]. Hence, its gap Chern number is well defined and given by the Chern number of that band: $\mathcal{C}_n^+ = (-1)^n$, as discussed in the main text. The gap Chern number of the pseudospin class “+” is given by the non-convergent series $\mathcal{C}_{\text{gap}}^+ = -1 + 1 - 1 \dots$, that results from summing the Chern numbers of all the negative frequency bands. Therefore, we conclude that the Hamiltonian decomposition in Eq. (S40) provides a precise meaning to this infinite sum. It corresponds to the sum of the gap Chern numbers of the partial Hamiltonians $\hat{\mathcal{H}}_n^+$. In agreement with the bulk-edge correspondence, the dispersion equation (S46) predicts that for each pseudospin and each quantum number n there is a single gapless unidirectional edge mode propagating in the gap of the corresponding partial Hamiltonian. It underlined here that, different from the global system, the operator $\hat{\mathcal{H}}_n^+$ has a well-defined topology, and hence its edge states are ruled by the bulk-edge correspondence. The n -th term in the series $\mathcal{C}_{\text{gap}}^+$ determines the edge state with quantum number n .

The direction of propagation of an edge state of $\hat{\mathcal{H}}_n^+$ is locked to the sign of the respective gap Chern number [S9], $\mathcal{C}_n^+ = (-1)^n$, in agreement with the numerical results. As an edge state with number n cannot scatter into waves with different n when the shape of the lateral boundary is deformed, the edge modes are topologically protected.

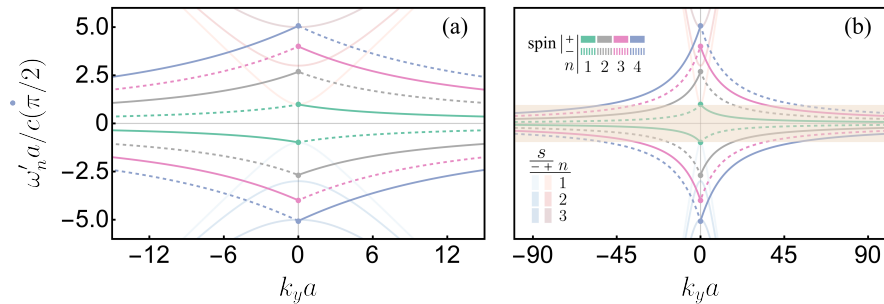


FIG. S5. (a) Frequency bands ω_n of bulk ($n < 4$) and edge ($n < 5$) waves as a function of the propagation constant k_y , for a normalized reactance $\chi_z = 0.12\omega a/c$. Red/Blue translucent tones refer to the positive/negative bulk states. Other colors concern the edge modes: green for $n = 1$, orange for $n = 2$, purple for $n = 3$ and pink for $n = 4$. Edge waves with pseudospin “+”/“−” are represented by solid/dashed bands. For a fixed pseudospin, the direction of propagation of the edge waves alternates as the quantum number n changes. For the same number n , the edge waves have opposite propagation directions for opposite pseudospins. (b) Range of k_y is extended. All edge states span the entire photonic band gap indicated by the beige rectangular region.

According to Eq. (S46), for any $n \in \mathbb{N}$, flipping the pseudospin is equivalent to flip the propagation direction of the edge wave along the y -axis. This is expected from electromagnetic reciprocity. It is also consistent with the fact that the Chern numbers associated with the "+" and "-" pseudospins differ from a minus sign: $C_n^- = -C_n^+$. As already mentioned, the direction of propagation of an edge wave is locked to the sign of the gap Chern number. It is also curious note that the edge modes are backward waves, and that the positive and negative frequency branches are joined at $k_y = \infty$, guaranteeing in this manner that the edge waves are gapless.

It is useful to note that Eqs. (S43) and (S44) give

$$\frac{k^2}{\kappa_n} \boldsymbol{\psi} = \left(-i \mathbf{k} \pm \frac{\omega_n}{c\kappa_n} (-1)^n \hat{\mathbf{z}} \times \mathbf{k} + \frac{k^2}{\kappa_n} \hat{\mathbf{z}} \right) e^{i\mathbf{k} \cdot \mathbf{r}}. \quad (\text{S47})$$

Hence, the full pseudospinors that represent edge waves propagating along the straight lateral wall are

$$\boldsymbol{\Psi}_n^\pm(\mathbf{r}, t) \propto \left(\sin[\kappa_n(z - a/2)] \left(-i \mathbf{k} \pm \frac{\omega_n}{c\kappa_n} (-1)^n \hat{\mathbf{z}} \times \mathbf{k} \right) + \frac{k^2}{\kappa_n} \cos[\kappa_n(z - a/2)] \hat{\mathbf{z}} \right) e^{-i\omega_n t} e^{ik_y y} e^{-\alpha_x x}. \quad (\text{S48})$$

Curiously, the above field structure is coincident with that of a bulk mode with index n but with a complex-valued wave-vector. Note that for a conservative waveguide ($\rho = 0$) one has $h_n = -e^{-i\kappa_n a}$ [see Eq. (S10)].

-
- [S1] W.-J. Chen, Z.-Q. Zhang, J.-W. Dong, and C. T. Chan, Symmetry-protected transport in a pseudospin-polarized waveguide, *Nature Communications* **6**, [10.1038/ncomms9183](#) (2015).
 - [S2] M. G. Silveirinha, $\mathcal{P} \cdot \mathcal{T} \cdot \mathcal{D}$ symmetry-protected scattering anomaly in optics, *Physical Review B* **95**, [10.1103/physrevb.95.035153](#) (2017).
 - [S3] J. A. Nelder and R. Mead, A simplex method for function minimization, *The Computer Journal* **7**, 308 (1965).
 - [S4] H. Shen, B. Zhen, and L. Fu, Topological band theory for non-hermitian hamiltonians, *Physical Review Letters* **120**, [10.1103/physrevlett.120.146402](#) (2018).
 - [S5] M. G. Silveirinha, Chern invariants for continuous media, *Physical Review B* **92**, [10.1103/physrevb.92.125153](#) (2015).
 - [S6] F. R. Prudêncio and M. G. Silveirinha, Ill-defined topological phases in local dispersive photonic crystals, *Phys. Rev. Lett.* **129**, [133903](#) (2022).
 - [S7] P.-S. Kildal, Definition of artificially soft and hard surfaces for electromagnetic waves, *Electronics Letters* **24**, 168 (1988).
 - [S8] P.-S. Kildal, Artificially soft and hard surfaces in electromagnetics, *IEEE Transactions on Antennas and Propagation* **38**, [1537](#) (1990).
 - [S9] M. G. Silveirinha, Proof of the bulk-edge correspondence through a link between topological photonics and fluctuation-electrodynamics, *Phys. Rev. X* **9**, [011037](#) (2019).